Propagation Characteristics in Indoor Office Scenario at 3.5 GHz

Jing Zeng†, Jianhua Zhang*†,
*Key Laboratory of Universal Wireless Communications, Ministry of Education,†Wireless Technology Innovation Institute
Beijing University of Posts and Telecommunications, P.O. box #92, China,100876
Email: zengjing@bupt.edu.cn

***Abstract*—This paper presents results from the measurement in indoor office scenario at 3.5 GHz. The measurement was performed using vertical-polarized dipole antennas (VDA) and omni-directional array (ODA). Three cases including corridor-to-corridor, corridor-to-room and room-to-room, have been measured and comprehensive propagation characteristics have been investigated. Based on the measurement, large-scale, delay and spatial models are built and compared with the standard models. Path loss turns out to be 3-5 dB smaller in indoor line-of-sight condition, while it is larger in non-line-of-sight condition because of the attenuation of concrete walls. Delay spread is the maximal in corridor-to-corridor case due to a strong reflection multipath component and angular spread in space domain is much larger than standard models in indoor scenario.**

I. INTRODUCTION

With the indoor data service increasing dramatically, more and more new techniques have been put forward to cope with indoor traffic explosion. Broadening bandwidth and improving spectrum efficiency are two ways. However, considering the shortage of frequency resource, finding sufficient and suitable frequency band is urgent to the future communication services. So higher frequency bands draw our attention. Recently, small cell enhancement for hotspot deployments in indoor scenario is proposed by the 3rd Generation Partner Project (3GPP) in TR 36.932 [1], with special focus on higher frequency bands, e.g., the 3.5 GHz band, to enjoy the more available spectrum and wider bandwidth. Besides, 3.5 GHz has been discussed to allocate in indoor deployment in China.

In real environments, the achievable capacity and performance depend to a large extent on the radio channel. So accurate channel models are of vital importance to system simulation. Path loss and shadow fading are key parameters to analyze indoor coverage; delay spread (DS) limits the length of cyclic prefix in Orthogonal Frequency-Division Multiplexing (OFDM) system; angular spread (AS) indicates the degree of dispersion in space domain. All these propagation characteristics should be modeled accurately. However, when frequency increases, radio wave becomes shorter in wavelength and suffers more power loss during the propagation so that the coverage area becomes smaller [2]. Furthermore, different indoor layouts have different propagation characteristics. Currently, the standard model International Telecommunication Union (ITU) M.2135 [3] only defines one scenario named indoor hotspot for the indoor environment. Indoor office scenario, as one of the typical and common indoor environment, defined as A1 in Wireless World Initiative New Radio (WINNER) II channel model [4], but its channel models are built based on the measurement at 2.45 GHz and 5.25 GHz.

The propagation environment is complicated in indoor scenario and many factors can have an impact on it, such as the materials of walls and ceiling, or whether the door is open or closed. To obtain realistic propagation characteristics, channel measurement is the most straightforward approach. So far, abundant measurements have been done in indoor scenarios at different frequency [5]–[7]. However, numerous discrepancies exist for the different carrier frequency and different layouts. So this establishes the necessity to precisely model indoor office environment at a certain frequency.

3.5 GHz band has been used in Worldwide Interoperability for Microwave Access (WIMAX) system, so most of the measurements reported at 3.5 GHz are about WIMAX radio channels [8], [9]. To our knowledge, the measurements conducted in cellular system at 3.5 GHz are so little in indoor scenario. [10] compares path loss models for suburban scenario at 2.3 GHz, 2.6 GHz and 3.5 GHz. [11] and [12] analyze multi-polarized statistics for outdoor-to-indoor and indoor-to-indoor channels at 3.5 GHz. The comprehensive channel models in indoor office scenario at 3.5 GHz are lacking, so more attention should be paid.

Thus, in this paper, propagation characteristics in indoor office scenario at 3.5 GHz is investigated. Three cases including corridor-to-corridor (C-C), corridor-to-room (C-R) and room-to-room (R-R), have been measured in detail. Comprehensive propagation characteristics, including path loss, shadow fading, DS and AS, have been analyzed and compared with standard models for the three cases. More underlying reasons are also analyzed.

The rest of this paper is organized as follows. Section II gives a description of the measurement campaign. Section III introduces the analysis methods of path loss, shadow fading, DS and AS. Detailed analysis results are shown in Section IV and Section V presents the relevant conclusions.

II. MEASUREMENT DESCRIPTION

A. Measurement System

To explore the comprehensive channel propagation characteristics, two types of antennas are used. One is vertical-polarized dipole antennas (VDA) and the other is omni-directional array (ODA). Electrobit Propsound Channel

TABLE I
MEASUREMENT PARAMETERS

Items	VPD	ODA
Central Frequency (GHz)	3.5	3.5
Bandwidth (MHz)	100	100
Chip Frequency (MHz)	50	50
Sampling Rate (Hz)	185.883	54.389
Length of PN Code	127	63
Emitting Power (dBm)	23	23
Number of Tx antennas	1	32
Number of Rx antennas	1	56
Height of Tx antenna (m)	2.1	2.1
Height of Rx antenna (m)	1.7	1.7

Sounder [13] was utilized to conduct our measurement, which sends binary pseudo-noise (PN) code. The central frequency is 3.5 GHz with 100 MHz bandwidth. More detailed parameters are listed in Table I.

B. Measurement Environment

The measurement was performed on the 7th floor of the research building in Beijing University of Posts and Telecommunications, which can be characterized as a typical indoor office scenario similar to the A1 scenario defined in WINNER II channel model. There are rooms located in both sides of the corridor. The inner blocked walls are made of reinforced. The room furnished with plenty of office workspaces, has a length of 10 meters and width of 8 meters. The corridor is 50 meters long, 2 meters wide and 2.2 meters high.

The field measurement plan is shown in Fig. 1. The red triangles represent the location of transmitter (Tx) antenna. Tx1 and Tx2 stand for the location in the corridor and room, respectively. The receiver (Rx) antenna is moving in the corridor and room at a walking speed along the yellow arrows. There is a long route in the corridor and three short routes in the room, and the exact moving distances have been marked in Fig. 1. When Tx and Rx are located in the corridor, it is C-C case. When Tx is located in the corridor while Rx is moving in the room, it represents C-R case. R-R case means that Tx and Rx are in the room. C-C and R-R cases belong to line-of-sight (LOS) condition while C-R case belongs to non-line-of-sight (NLOS) condition. For VDA, three cases have been measured, which are C-C, R-R and C-R. For ODA, only C-C and R-R cases are measured. Field measurements have been done repeatedly. The field environments during ODA measurement are shown in Fig. 2 and Fig. 3.

III. ANALYSIS METHODS

After the field measurements, two procedures need to be done: first, obtaining channel impulse response (CIR) by slide correlating the received signal with a synchronized copy of the PN sequence; then extracting channel parameters from CIR, including large-scale, delay and spatial parameters.

A. Large-Scale Parameters

Define $h(t, \tau_l)$ as CIR and it is averaged in time domain under the assumption of wide-sense stationary uncorrelated

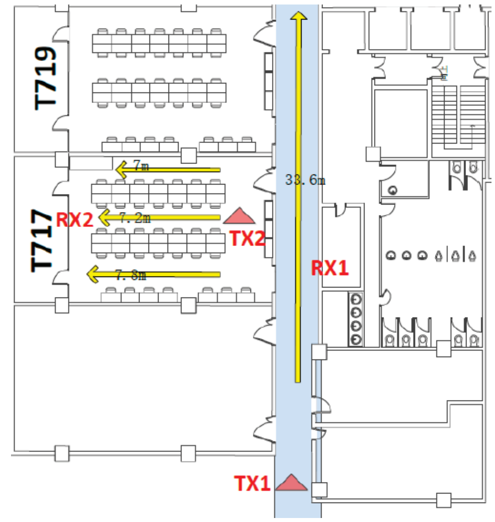

Fig. 1. The Field Measurement Plan in Indoor Office Scenario

Fig. 2. The Propagation Environment in C-C Case for ODA

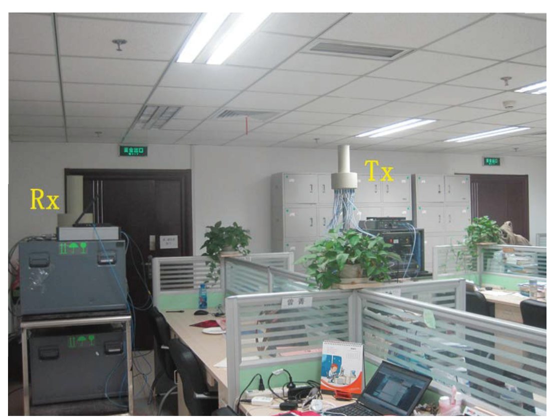

Fig. 3. The Propagation Environment in R-R Case for ODA

scattering (WSSUS), which is shown as below.

$$h_{av}(\tau_l) = E_t\left[h(t,\tau_l)\right] \tag{1}$$

where E_t denotes the average in time domain.

Then power delay profile (PDP) is calculated by

$$P(\tau_l) = \left|h_{av}(\tau_l)\right|^2 \tag{2}$$

For a PDP, to filter the noise, the threshold is set 20 dB below the strongest multipath component (MPC), then measured path loss values are calculated in dB as

$$PL = -10\log 10(\sum_l |P(\tau_l)|) + G_{Tx} + G_{Rx} \tag{3}$$

where G_{Tx} and G_{Rx} denote the gain of Tx and Rx antenna, respectively.

So far, almost all the large scale fading models are based on single-slope log-distance model as (4).

$$PL(d) = PL_0 + 10n \cdot \log_{10} d + X_\sigma \tag{4}$$

where PL_0 represents the intercept, d is the separation distance between Tx and Rx, and n denotes the path loss exponent which indicates the rate at which path loss increases with distance. The shadow fading is modeled by a zero-mean Gaussian random variable X_σ with standard deviation σ.

B. Delay Parameters

For delay parameters, mean excess delay is defined as the first moment of PDP and calculated by (5). It represents the MPCs' average propagation delay compared to the arrival of the first MPC.

$$\tau_{mean} = \frac{\sum_l P(\tau_l) \cdot \tau_l}{\sum_l P(\tau_l)} \tag{5}$$

Rms DS is defined as the root square of the second central moment of PDP and calculated by (6). The dispersion degree of the MPCs in delay domain is given by

$$\tau_{rms} = \sqrt{\frac{\sum_l P(\tau_l) \cdot (\tau_l - \tau_{mean})^2}{\sum_l P(\tau_l)}} \tag{6}$$

Max excess delay $\tau_{\max}$, represents the delay duration between the first and last MPC above the threshold.

C. Spatial Parameters

ODA is used to conduct measurement for spatial parameters and Tx has 32 dual-polarized patch elements while Rx has 56. Then space alternating generalized expectation (SAGE) maximization algorithm is used to estimate the parameters in spatial domain. In our measurement, the angle of departure (AOD) represents the angle radiated from Tx and the angle of arrival (AOA) is used to describe the waves reached to Rx. AS, the second moment of the propagation angles, can be calculated with the same method as that of DS. In order to avoid the problem of angular blur, a new method in 3GPP spatial channel model (SCM) channel model [14] is adopted for the calculation of circular angular spread (CAS). Taking AOD for example, ϕ_ℓ is the AOD of the ℓ_{th} path. $\varphi_\ell(\Delta) = \phi_\ell + \Delta$. Then AS is defined as the minimum value for all offset angle Δ.

$$\sigma_{rms} = \min_{\Delta} \sigma_{rms}(\Delta) = \sqrt{\frac{\sum_{\ell=1}^{L} \left(\varphi_\ell(\Delta) - \mu(\Delta)\right)^2 p_\ell}{\sum_{\ell=1}^{L} p_\ell}} \tag{7}$$

and $\mu(\Delta)$ is

$$\mu(\Delta) = \frac{\sum_{\ell=1}^{L} \varphi_\ell(\Delta) p_\ell}{\sum_{\ell=1}^{L} p_\ell} \tag{8}$$

where $\varphi_\ell(\Delta)$ and $\varphi_\ell(\Delta) - \mu(\Delta)$ are normalized into the range of $[-\pi, \pi]$.

$$\varphi = \begin{cases} \varphi + 2\pi & if\ \varphi < -\pi \\ \varphi & if\ |\varphi| \le \pi \\ \varphi - 2\pi & if\ \varphi > \pi \end{cases} \tag{9}$$

IV. Analysis Results

A. Path Loss and Shadow Fading

Large-scale models are vital to analyze the coverage, planning and optimization of wireless system. We use VDA to obtain path loss and shadow fading models.

Three different cases are measured for VDA, which are C-C, C-R and R-R. In C-C case, from Fig. 4(a), the blue dots represent the realistic measured data and the red curve is the fitted model. Path loss exponent is 1.76, which is smaller than 2 in free space model. Besides, path loss is 2-3 dB smaller than standard model ITU M.2135 and WINNER II model, which indicates the existence of waveguide effect. Because of it, more reflections happen, so the received signals strengthen and path loss becomes smaller. Shadow fading is fitted with the standard normal distribution and standard deviation is 3.4. It is shown in Fig. 5.

In R-R case, path loss is 5 dB smaller than standard models, shown in Fig. 4(b). It has a path loss exponent of 1.46, indicating path loss increases with distance slowly. Since the room has a small area, the range of distance between Tx and Rx is smaller than that in the corridor. At a closer distance, most of the energy can be received at Rx directly, so path loss turns out smaller.

In NLOS condition from corridor to room, signals have to transmit through concrete walls and the attenuation is severe. From Fig. 4(c), path loss is much larger than standard models, resulting from the attenuation of concrete walls. For ITU M.2135 model, the NLOS condition means there is no LOS component between Tx and Rx, but signals don't go through heavy wall transmitting to Rx.

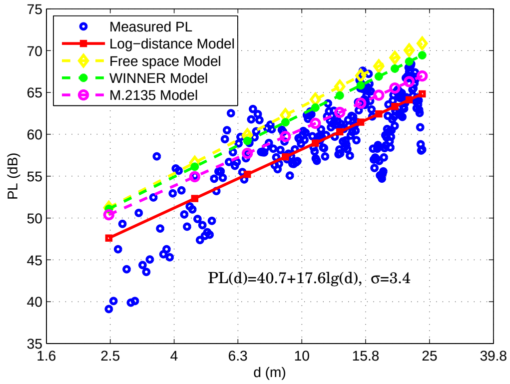

(a) C-C Case

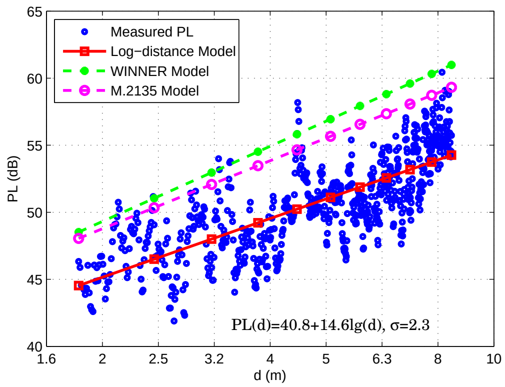

(b) R-R Case

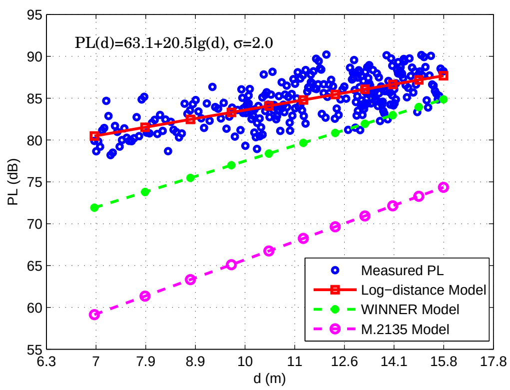

(c) C-R Case

Fig. 4. Path Loss Models for Three Cases

From the above, in LOS condition, we can revise standard models subtly according to simulation conditions, but the attenuation of concrete walls can't be ignored in NLOS condition .

Finally, the large-scale models for these three scenarios have been tabulated and shadow fading is also given in Table II.

B. Delay Characteristics

Next we analyze delay parameters. Mean excess delay, rms DS and maximum excess delay have been calculated and listed in Table III.

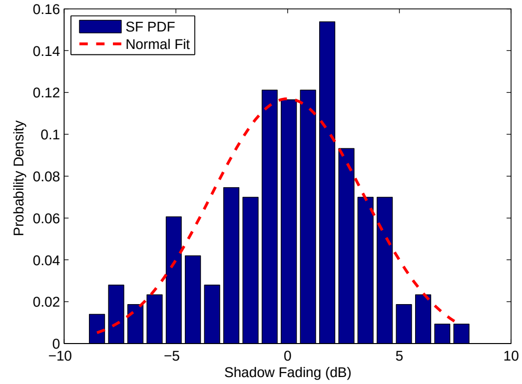

Fig. 5. Shadow Fading in C-C Case

TABLE II
PATH LOSS MODELS FOR THREE CASES

Case	Models
C-C	$PL(d) = 40.7 + 17.6\log(d)$, σ=3.4
C-R	$PL(d) = 63.1 + 20.5\log(d)$, σ=2
R-R	$PL(d) = 40.8 + 14.6\log(d)$, σ=2.3

TABLE III
DELAY PARAMETERS FOR THREE CASES

Case	τ_{mean} [ns]	τ_{rms} [ns]	$\tau_{\max}$ [ns]
C-C	34	33	185
C-R	33	20	100
R-R	37	20	144

There is nearly no difference of mean excess delay for these three cases. However, from Table III, rms DS in C-C case is the maximal one. To find out reasons, the PDP of one snapshot in C-C case is shown in Fig. 6. There are two evident high peaks in Fig. 6, which does not appear in other cases. It has been circled in red and demonstrates there exists another strong reflection MPC besides the strongest one. Since the corridor is narrow and long, the complicated propagation environment and strong multipath effect lead to this phenomenon. In R-R case, the unique peak is wider than that in Fig. 6, showing most of energy has been received, but no evident strong reflection MPCs appear. So rms DS is the maximal in C-C case.

For A1 scenario in WINNER II model, rms DS are 38 and 25 ns, respectively, in LOS and NLOS condition. It is consistent with our measured results.

C. Spatial Characteristics

Finally, spatial parameters are analyzed. ODA has been applied in two cases, C-C and R-R. For both AOA and AOD, the statistical values of CAS in two cases are depicted in Table IV. μ and σ are the parameters of log-normal distributions.

From Table IV, in these two cases, AS of both AOA and AOD are larger than that in standard models. One snapshot is randomly chosen to seek a cause. The snapshot is in R-R case and its joint AOA-AOD plot is shown in Fig. 7. X-axis and Y-axis represent AOA and AOD in rad, respectively. The

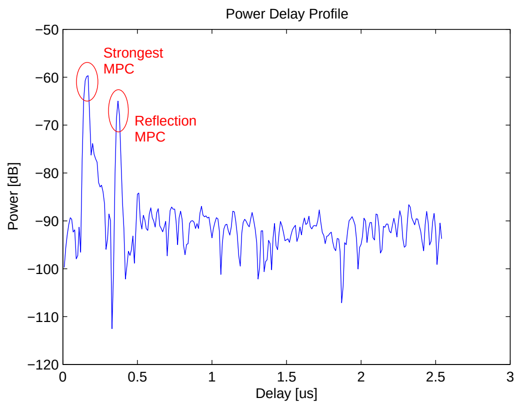

Fig. 6. PDP of One Snapshot in C-C Case

TABLE IV
SPATIAL PARAMETERS FOR TWO CASES

		C2C	R2R	M.2135(InH)	WINNER (A1)
AOA Spread	μ	1.86	1.9	1.60	1.64
$\log_{10}([°])$	σ	0.32	0.35	0.18	0.31
AOD Spread	μ	1.93	1.94	1.62	1.65
$\log_{10}([°])$	σ	0.37	0.39	0.22	0.26

size of circles are proportional to the power of MPCs. From Fig. 7, the strongest MPCs centralize in zero degree in the red ellipse for both AOA and AOD, close to LOS direction, but the energy is quite disperse in space for there are lots of MPCs in other degrees. Reviewing Fig. 3, the room is furnished with plenty of office workspaces and so many scatters exist, leading to large AS.

The results given above indicate that more MIMO technique should be explored in indoor scenario because of the larger AS, which brings about high system capacity.

V. CONCLUSION

We presented the results from the measurement in indoor office scenario. This frequency range and application scenario is of great importance to indoor enhance technique. Three cases at 3.5 GHz have been measured for VPD and ODA to obtain large-scale, delay and spatial parameters. Quite a large amount of valuable conclusions have been drawn.

In LOS condition, path loss is 3-5 dB smaller than standard models, so we can revise standard models subtly according to simulation conditions. In addition, path loss is larger in NLOS condition so that we can't ignore the attenuation of concrete walls. As for delay parameters, they are consistent with the results of A1 scenario in WINNER II model. In C-C case, a strong reflection MPC exist, leading to the maximum rms DS and max excess delay. The statistical spatial parameters of both AOA and AOD are much larger than that in standard models, indicating a high degree of available spatial diversity. We should take advantage of these valuable conclusions in indoor scenario for better system design, simulation and evaluation.

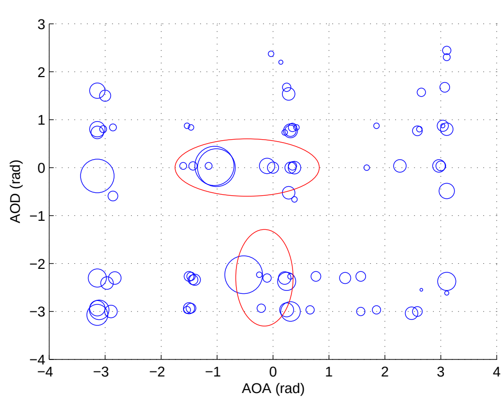

Fig. 7. Joint AOA-AOD Plot for One Snapshot

VI. ACKNOWLEDGEMENTS

The research is supported by China Key Projects in the National Science and Technology (NO.2012ZX03006003-003) and National Science and Technology Major Project of the Ministry of Science and Technology (NO.2012ZX03001043-009).

REFERENCES

[1] *Scenarios and Requirements for Small Cell Enhancements for E-UTRA and E-UTRAN (Release 12)*, V12.0.0 ed., 3GPP TR 36.932.
[2] D. Lu and D. Rutledge, "Investigation of indoor radio channels from 2.4 ghz to 24 ghz," in *Proc. IEEE Antennas and Propagation Society Int. Symp*, vol. 2, 2003, pp. 134–137.
[3] *Guidelines for evaluation of radio interface technologies for IMT-Advanced*, ITU-R Report M.2135, Nov. 2008.
[4] *WINNER II Channel Models*, IST-WINNER II Deliverable 1.1.2, 2008.
[5] D. Laselva, X. Zhao, J. Meinila, T. Jamsa, J. P. Nuutinen, P. Kyosti, and L. Hentila, "Empirical models and parameters for rural and indoor wideband radio channels at 2.45 and 5.25 ghz," in *Personal, Indoor and Mobile Radio Communications, 2005. PIMRC 2005. IEEE 16th International Symposium on*, vol. 1, 2005, pp. 654–658.
[6] X. Nie, J. Zhang, Y. Zhang, G. Liu, and Z. Liu, "An experimental investigation of wideband mimo channel based on indoor hotspot nlos measurements at 2.35ghz," in *Global Telecommunications Conference, 2008. IEEE GLOBECOM 2008. IEEE*, 2008, pp. 1–5.
[7] M.-D. Kim, H. K. Kwon, B. S. Park, J.-J. Park, and H. K. Chung, "Multi-path channel parameters based on indoor hotspot channel measurements at 3.7ghz," in *Advanced Communication Technology (ICACT), 2011 13th International Conference on*, 2011, pp. 579–583.
[8] B. Belloul, A. Aragon-Zavala, and S. Saunders, "Measurements and comparison of wimax radio coverage at 2.5 ghz and 3.5 ghz," in *Antennas and Propagation, 2009. EuCAP 2009. 3rd European Conference on*, 2009, pp. 3287–3291.
[9] J. Roldao and P. Pinho, "Bi-dimensional characterization of a wimax radio channel at 3.5ghz," in *Antennas and Propagation (EuCAP), 2010 Proceedings of the Fourth European Conference on*, 2010, pp. 1–5.
[10] S. Kun, W. Ping, and L. Yingze, "Path loss models for suburban scenario at 2.3ghz, 2.6ghz and 3.5ghz," in *Antennas, Propagation and EM Theory, 2008. ISAPE 2008. 8th International Symposium on*, 2008, pp. 438–441.
[11] A. Panahandeh, F. Quitin, J. M. Dricot, F. Horlin, C. Oestges, and P. De Doncker, "Multi-polarized channel statistics for outdoor-to-indoor and indoor-to-indoor channels," in *Vehicular Technology Conference (VTC 2010-Spring), 2010 IEEE 71st*, 2010, pp. 1–5.
[12] A. Panahandeh, F. Quitin, J. Dricot, F. Horlin, C. Oestges, and P. De Doncker, "Orientation-free xpd and cpr model in outdoor-to-indoor and indoor-to-indoor channels," in *Antennas and Propagation (EuCAP), 2010 Proceedings of the Fourth European Conference on*, 2010, pp. 1–5.
[13] *Propsound multidimensional channel sounder, Elektrobit Ltd. [Online]. Available:http://www.propsim.com.*
[14] *Technical Specification Group Radio Access Networks; Spatial Channel Model for MIMO Simulations (Release 6)*, V6.1.0 ed., 3GPP TR 25.996.